


REPORT



Generation and *in vivo* characterization of a novel high-affinity human antibody targeting carcinoembryonic antigen

Louis Plüss ^{a,b}, Frederik Peissert ^a, Abdullah Elsayed ^{a,b}, Giulia Rotta ^a, Jonas Römer ^b, Sheila Dakhel Plaza ^a, Alessandra Villa ^a, Emanuele Puca ^a, Roberto De Luca^a, Annette Oxenius ^b, and Dario Neri ^{a,b,c}

^aPhilochem AG, Libernstrasse 3, Otelfingen, Switzerland; ^bDepartment of Biology, Swiss Federal Institute of Technology (ETH Zürich), Zurich, Switzerland; ^cPhilogen SpA, Località Bellaria, Sovicille, Italy

ABSTRACT

There are no effective treatment options for most patients with metastatic colorectal cancer (mCRC). mCRC remains a leading cause of tumor-related death, with a five-year survival rate of only 15%, highlighting the urgent need for novel pharmacological products. Current standard drugs are based on cytotoxic chemotherapy, VEGF inhibitors, EGFR antibodies, and multikinase inhibitors. The antibody-based delivery of pro-inflammatory cytokines provides a promising and differentiated strategy to improve the treatment outcome for mCRC patients. Here, we describe the generation of a novel fully human monoclonal antibody (termed F4) targeting the carcinoembryonic antigen (CEA), a tumor-associated antigen overexpressed in colorectal cancer and other malignancies. The F4 antibody was selected by antibody phage display technology after two rounds of affinity maturation. F4 in single-chain variable fragment format bound to CEA in surface plasmon resonance with an affinity of 7.7 nM. Flow cytometry and immunofluorescence on human cancer specimens confirmed binding to CEA-expressing cells. F4 selectively accumulated in CEA-positive tumors, as evidenced by two orthogonal *in vivo* biodistribution studies. Encouraged by these results, we genetically fused murine interleukin (IL) 12 to F4 in the single-chain diabody format. F4-IL12 exhibited potent antitumor activity in two murine models of colon cancer. Treatment with F4-IL12 led to an increased density of tumor-infiltrating lymphocytes and an upregulation of interferon γ expression by tumor-homing lymphocytes. These data suggest that the F4 antibody is an attractive delivery vehicle for targeted cancer therapy.

ARTICLE HISTORY

Received 20 February 2023
Revised 9 May 2023
Accepted 22 May 2023

KEYWORDS


CEA; colorectal cancer; immunocytokine; interleukin-12; monoclonal antibodies; phage display technology; protein engineering; tumor targeting

Introduction

Colorectal cancer (CRC) is the third most common cancer worldwide, with almost two million newly diagnosed cases per year.¹ The introduction of extensive screening programs led to earlier detection of CRC in many patients.² Nevertheless, over 20% of patients are diagnosed after the malignant cells have metastasized to other tissues, such as the liver, lungs, lymph nodes, peritoneum, or soft tissues.³ Unresectable metastatic CRC (mCRC) is conventionally treated with a cocktail of chemotherapeutic agents, often based on 5-fluorouracil, capecitabine, irinotecan, and/or oxaliplatin.⁴ Patients with *KRAS/NRAS/BRAF* wild-type tumors typically receive combination regimens of antibody-based therapeutics targeting angiogenic and tumor growth factors (e.g., anti-EGFR, anti-VEGF antibodies).⁴ Nonetheless, the prognosis for mCRC patients remains very poor, with an overall survival rate of less than 15%, highlighting the urgent need for alternative treatment strategies.⁵ Immune checkpoint inhibitors have shown clinical activity in various malignancies.^{6–11} However, activity in mCRC patients is generally low, with exceptions made for a small proportion of subjects with a high level of microsatellite instability or changes to a mismatch repair gene who benefit from treatment with checkpoint inhibitors.¹²

Monoclonal antibodies have many pharmaceutical applications and are increasingly used for anti-cancer strategies.¹³ Certain antibody-based therapeutics may allow immunologically “cold” tumors to become “hot,” boosting the antitumor immune response.¹⁴ For example, a tumor-homing antibody moiety may facilitate the delivery of immunostimulatory cytokines to the neoplastic mass,^{15–17} increasing the intratumoral density and activity of T cells and natural killer (NK) cells against malignant cells.^{18,19} In the context of mCRC, carcinoembryonic antigen (CEA) represents the most validated accessible cell surface antigen for antibody-based pharmacodelivery applications. Immunohistochemical evaluations in mCRC specimens have shown that CEA is overexpressed in 98.8% of tumors.²⁰ CEA is a glycosylphosphatidylinositol-anchored membrane protein consisting of seven Ig-like domains [Supplementary Figure S1A].²¹ In healthy organs, CEA expression is restricted to the apical surface of mature enterocytes,²² making it virtually inaccessible for circulating antibodies. In malignant cells, the polarity of CEA expression is lost and the antigen becomes exposed to the vasculature and lymphatic system.²³ This selective accessibility in cancer was confirmed in numerous Nuclear Medicine studies, in which radiolabeled CEA-targeting antibodies localized to tumor

CONTACT Dario Neri  dario.neri@philogen.com  Philochem AG, Libernstrasse, Otelfingen 3, 8112, Switzerland

 Supplemental data for this article can be accessed online at <https://doi.org/10.1080/19420862.2023.2217964>.

© 2023 Philochem AG. Published with license by Taylor & Francis Group, LLC.

This is an Open Access article distributed under the terms of the Creative Commons Attribution-NonCommercial License (<http://creativecommons.org/licenses/by-nc/4.0/>), which permits unrestricted non-commercial use, distribution, and reproduction in any medium, provided the original work is properly cited. The terms on which this article has been published allow the posting of the Accepted Manuscript in a repository by the author(s) or with their consent.

lesions with low background in healthy tissues.^{24–26} Shedding of overexpressed CEA results in increased levels of the antigen in circulation and CEA is widely used as a biomarker to monitor response to treatment or disease recurrence.^{27,28} However, serum levels of CEA in mCRC patients are usually in the sub-nanomolar or even sub-picomolar range and the proportion of antibody therapeutics that may be trapped in serum is believed to be minimal.²⁷

A number of CEA-targeting biopharmaceuticals have already been developed and tested in clinical trials, including radiolabeled antibodies and antibody-drug conjugates.^{29,30} MEDI-565 (AMG 211) is a bispecific T-cell engager consisting of a humanized anti-CEA antibody fused to the deimmunized anti-CD3 antibody diL2K.³¹ The product showed promising anti-cancer activity in preclinical models of cancer.³² However, in clinical studies, the product did not induce objective responses in patients suffering from gastrointestinal adenocarcinomas. The anti-tumor activity of MEDI-565 was likely affected by high anti-drug antibody (ADA) titers that were reported in most treated patients.^{33,34} It is well known that ADAs not only increase the risk of hypersensitivity reactions, but can also alter the pharmacodynamic and pharmacokinetic properties of protein-based therapeutics. It is therefore important to generate fully human products which are not immunogenic in patients.

Here, we describe the generation and validation of a novel fully human antibody (termed F4) specific to the N-terminal domain of CEA (CEA(N)). The parental clone G9 was selected from a synthetic human antibody phage display library, previously used to isolate novel antibodies against various targets.^{35–37} The high-affinity antibody F4 was isolated after two rounds of affinity maturation, which were necessary in order to achieve the desired performance in *in vivo* tumor targeting applications. When the F4 antibody was fused to murine interleukin (IL)-12 in single-chain diabody format, the resulting F4-IL12 fusion protein induced significant tumor growth regression in two murine models of cancer. *Ex vivo* analysis of treated mice revealed an increase in tumor infiltration of lymphocytes and an upregulation of interferon (IFN) γ expression by tumor-homing T cells. These data suggest that the fully-human F4 antibody may serve as a delivery vehicle for the generation of selective antibody-based cancer therapeutics.

Results

Isolation and characterization of antibodies specific to human CEA

CEA(N), used as a target for antibody phage display selection, was expressed in Chinese hamster ovary (CHO) cells and purified to homogeneity by affinity chromatography. An AviTag[®] was introduced at the N-Terminus of the recombinant antigen to allow site-specific biotinylation. SDS-PAGE and size exclusion chromatography (SEC) confirmed that the antigen was homogenous and of the expected size [Supplementary Figure S1B].

The G9 antibody, specific to CEA(N), was isolated by phage display technology from a large, fully human

synthetic antibody library. Binding kinetics were improved by selecting new clones (F7 and F4) from affinity maturation libraries based on the parental clone, with sequence variability restricted to the complementarity-determining region (CDR) 1 or CDR2 loops of the variable heavy (V_H) and variable light (V_L) domains [Supplementary Figure S1C].

Monomeric single-chain variable fragment (scFv) preparations of G9, F7, and F4 were analyzed by surface plasmon resonance (SPR), revealing dissociation constant (K_D) values of 640 nM, 50 nM, and 7.7 nM, respectively. [Figure 1A and Supplementary Figure S2A]. The three clones were subcloned into IgG and diabody format for further characterization [Supplementary Figure S2B-C]. Binding to CEA(N) was retained, as evidenced by SPR [Supplementary Figure S3A-B].

Characterization of anti-CEA antibodies by flow cytometry and immunofluorescence

The binding of the new antibodies in IgG format to CEA on the cell surface was confirmed by flow cytometry on the CEA-transfected murine cell line CT26 and on the human colon carcinoma cell lines LS174T and HT-29 [Figure 1B and Supplementary Figure S3C]. G9 showed moderate binding to CT26-CEA cells in high concentrations. The affinity-matured antibodies showed improved binding with functional affinity (K_D^{app}) values of 770 pM and 290 pM for F7 and F4, respectively. No binding was observed on CEA-negative CT26 wild-type cells [Figure 1B].

Immunofluorescence studies confirmed the binding of G9, F7, and F4 to human CRC xenografts. On LS174T tumor sections (high CEA expression), G9 showed a weak signal, while F7 and F4 strongly stained the cognate antigen [Figure 1C]. On the HT-29 tumor specimens (intermediate CEA expression), F4 stood out as the best-performing antibody [Supplementary Figure S3D]. No signal was obtained upon staining with the negative control antibody (KSF), specific for an irrelevant antigen [Supplementary Figure S3E].

F4 was further studied by immunofluorescence analysis on a tissue microarray containing different human cancer samples and their corresponding healthy tissues and on three additional human colon cancer sections. The previously described antibody Sm3E was used as a positive control. The F4 antibody detected CEA with a similar intensity to the one obtained with the Sm3E antibody on lung, pancreatic, and all tested colon tumors [Figure 2 and Supplementary Figure S4]. No signal was obtained upon staining the healthy organs or using the negative control antibody KSF [Figure 2 and Supplementary Figure S5].

Other CEA-related cell adhesion molecules (CEACAMs) have highly conserved N-terminal domains to CEA, especially CEACAM1, and CEACAM6. The specificity of the F4 antibody to CEA was confirmed by flow cytometry on transiently antigen-expressing CHO cells, as no binding was detected on CEACAM1- and CEACAM6-expressing cells [Supplementary Figure S6].

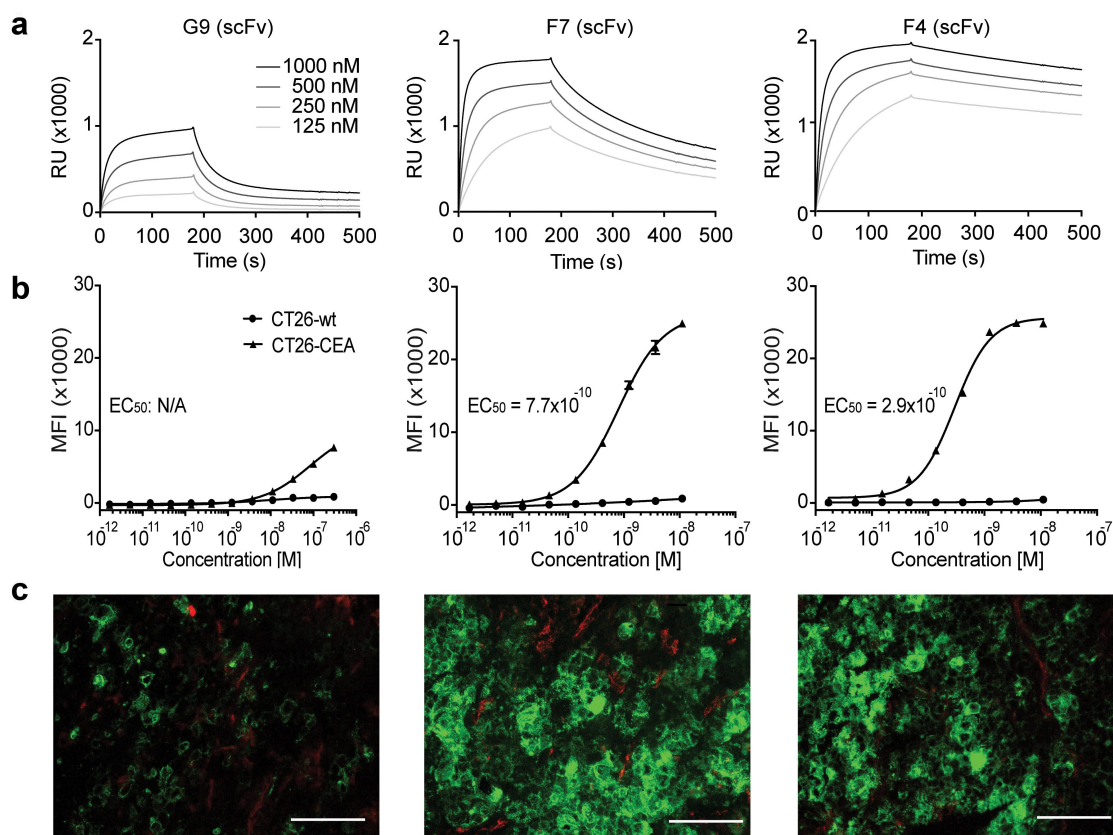


Figure 1. *In vitro* characterization of new anti-CEA antibodies. (a) SPR sensorgram of G9, F7, and F4 in a scFv format. K_D values were calculated to be 640 nM, 50 nM, and 7.7 nM, respectively. (b) Flow cytometry analysis with the new antibodies in IgG format on CEA-expressing CT26 cells and on CEA-negative CT26 wild-type cells. (c) Immunofluorescence staining with IgG formats on the human colon adenocarcinoma xenograft LS174T. Anti-CEA antibodies were detected in green. Blood vessels were detected by CD31 staining (red). 20× magnification, scale bars = 100 μm.

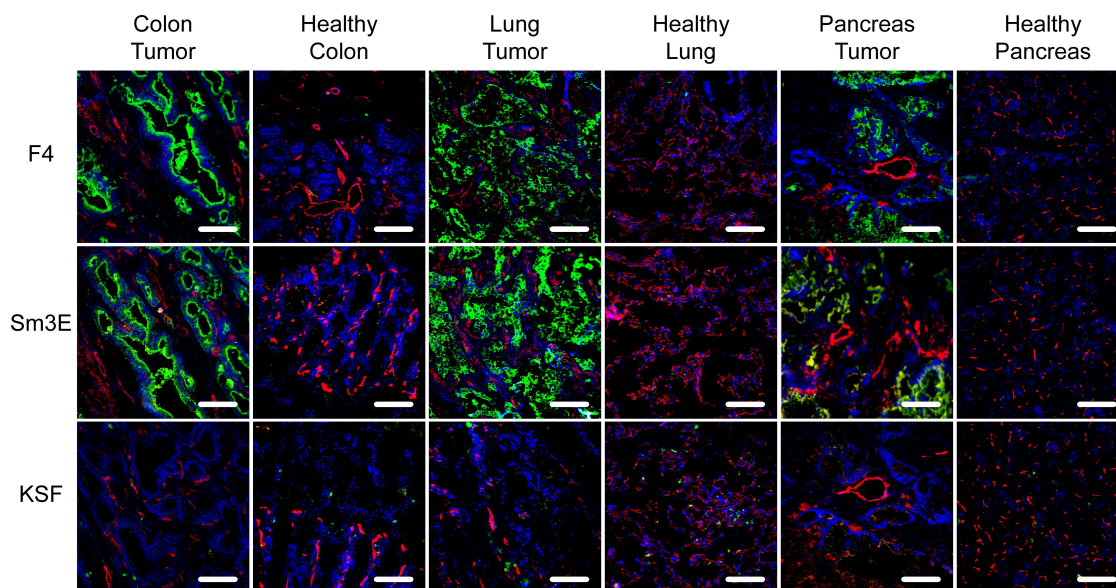


Figure 2. Immunofluorescence analysis of human cancer sections. Human tissue microarrays with cancer sections and corresponding healthy controls were analyzed by immunofluorescence analysis with F4, the positive control Sm3E, and an irrelevant isotype control (KSF). Antibody binding was detected in green. Blood vessels were detected with CD31 staining (red) and nuclei with DAPI (blue). 20× magnification, scale bars = 100 μm.

Immunofluorescence-based biodistribution analysis

The tumor-homing properties of G9, F7, and F4 were evaluated by immunofluorescence-based biodistribution analysis in LS174T tumor-bearing BALB/c nude mice. 200 μg fluorescein

isothiocyanate (FITC)-labeled IgG were injected intravenously into the lateral tail vein. Twenty-four hours post-injection, mice were sacrificed, and organs and tumors were harvested for further examination by immunofluorescence. F4 was

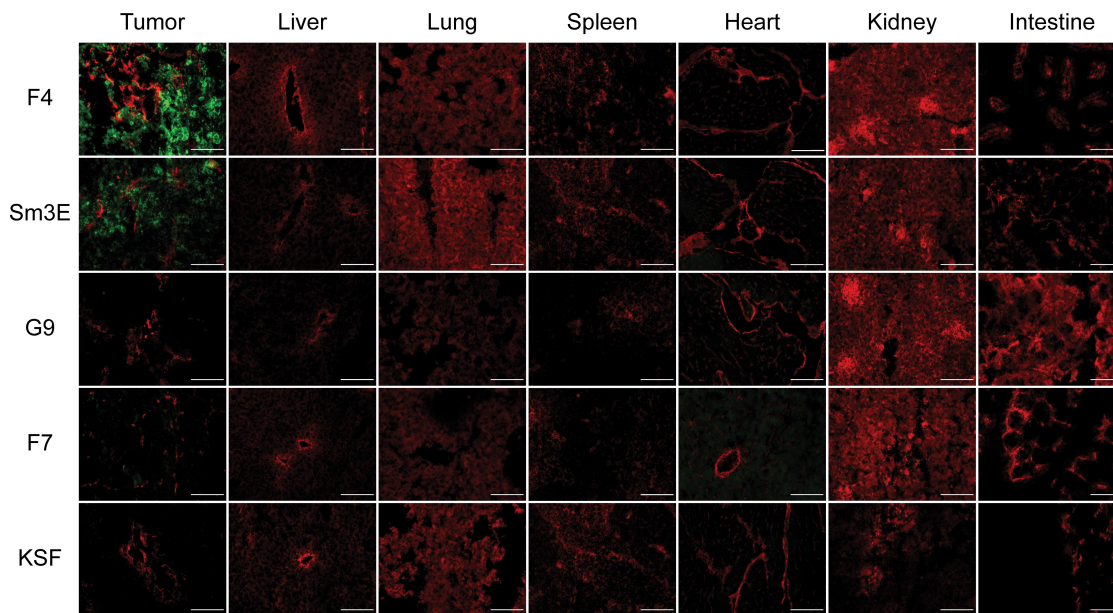


Figure 3. *Ex vivo* immunofluorescence-based biodistribution analysis. Immunofluorescence analysis assessed tumor targeting of new anti-CEA antibodies in IgG format. Two hundred micrograms of IgG-FITC were injected intravenously into LS174T-bearing mice. Tumors were excised 24 hours after injection. IgG-FITC was detected in green; blood vessels were detected through CD31 staining (red). 20× magnification, scale bars = 100 μ m.

found to selectively localize in the tumor, while no signal was detected in healthy organs. A similar result was obtained with the positive control antibody Sm3E. Despite an affinity of 50 nM, F7 showed only minimal uptake in the tumor, indicating that high affinity is required to achieve selective biodistribution [Figure 3]. The low-affinity antibody G9 and the KSF antibody, used as a negative control, revealed no staining in all organs. In line with previous studies performed by our group, the liver uptake of IgGs, which is usually observed in radio-labeled biodistribution studies with full-length IgGs, was not detectable in this experiment.^{35,36}

Quantitative biodistribution with radio-labeled diabodies

The *in vivo* tumor-targeting performance of the selected anti-CEA antibodies was further analyzed in a quantitative biodistribution experiment using ¹²⁵I-labeled diabodies. Antibodies were injected intravenously into LS174T tumor-bearing BALB/c nude mice. After 24 hours, mice were sacrificed, organs were harvested, and the radioactivity of the tumor, blood, and organs was measured. F4 was able to selectively localize in the neoplastic lesions, with a tumor-to-blood ratio of more than 8:1. Consistent with the immunofluorescence-based biodistribution experiment, modest accumulation in tumors was observed for the G9 and F7 antibodies [Figure 4].

Therapy studies with F4 fused to IL12

Encouraged by the selective tumor-homing properties of F4, we generated a fusion protein based on the F4 antibody in

single-chain diabody format, fused to the murine IL12 [Figure 5A]. F4-IL12 expressed with a yield of 13 mg/L of TGE, with clean bands in SDS-PAGE of the expected size and no signs of aggregation in the SEC profile. The protein showed excellent stability, exhibiting an unchanged SEC profile after a four-day incubation at 37°C [Supplementary Figure S7]. Retained functionality of the F4 and IL12 moieties was shown by SPR on a CEA(N) coated sensor chip and in a cellular IFN γ release assay on isolated murine splenocytes [Figure 5B-C]. The therapeutic efficacy of F4-IL12 was tested in different murine models of colorectal cancer. In mice bearing subcutaneous (s.c.) tumors of CEA-transfected CT26 cells, three injections of 12 μ g F4-IL12 led to significant tumor regression with a complete response in 33% of tested animals. No comparable results were achieved with untargeted IL12 (i.e., KSF-IL12) [Figure 5D-E]. These findings were confirmed in two additional studies in the more aggressive C51 model, with a dosing regimen of 3 \times 12 μ g and 4 \times 6 μ g, respectively, resulting in significant tumor growth retardation compared to mice treated with untargeted IL12 [Figure 5G-H and Supplementary Figure S8A]. F4-IL12 was well tolerated, as evidenced by the absence of body weight loss [Figure 5F-5I and Supplementary Figure S8B].

Ex vivo tumor analysis after treatment with F4-IL12

To analyze the mechanism of action of F4-IL12, tumors were excised 48 hours after the third injection, and infiltration of lymphocytes into the tumor mass was assessed by immunofluorescence. In both models, an increased density of NK cells and CD4⁺ T cells could be observed upon treatment with F4-IL12. No signal was obtained when stained for regulatory T cells. No increase in lymphocyte density was observed

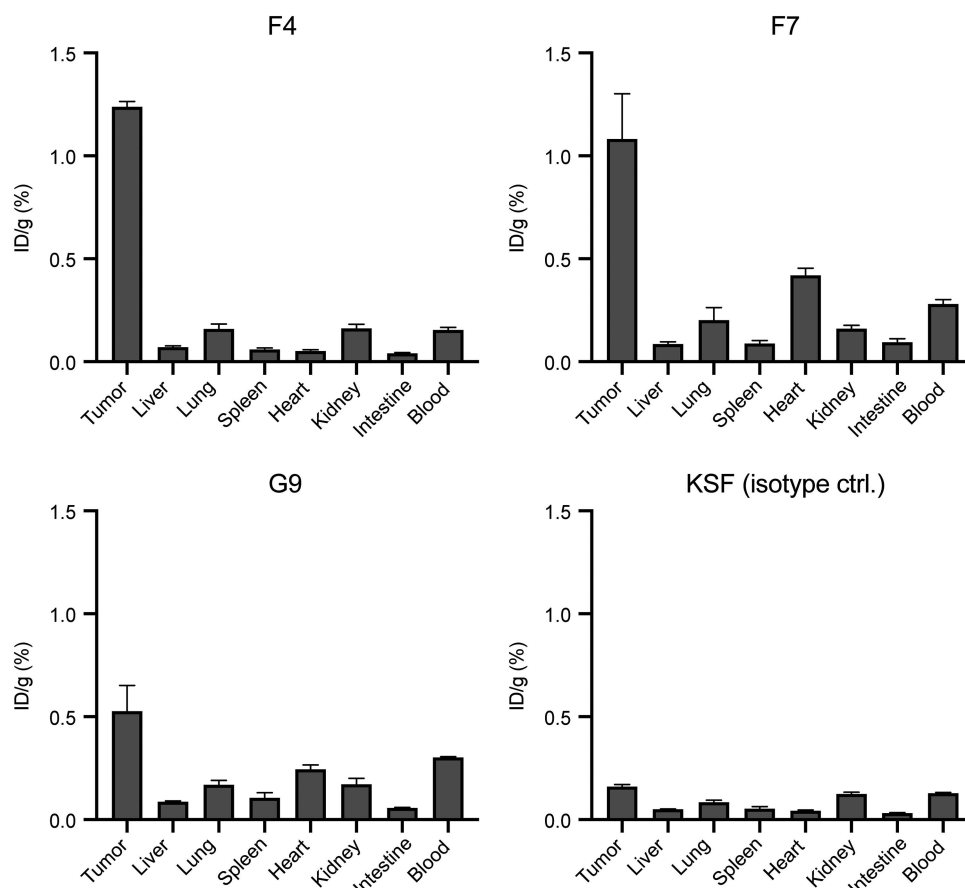


Figure 4. Quantitative biodistribution with radiolabeled anti-CEA antibodies in diabody format. Quantitative biodistribution analysis of radio iodinated anti-CEA diabodies in BALB/c nude mice bearing subcutaneous LS174T colon adenocarcinomas. Organs were harvested 24 hours after intravenous injection, and radioactivity was quantified. Results are shown as the percentage of injected dose per gram (ID/g (%)). Error bars = SEM; $n = 4$.

upon treatment with untargeted IL12, compared to mice treated with saline only [Figure 6A and Supplementary Figure 8C].

The tumor-homing T cells in the C51 model were additionally analyzed by flow cytometry. Both CD4⁺ and CD8⁺ T cells showed a significant increase in IFN γ expression. Also, the expression of PD-1, perforin, granzyme B, and the CD8⁺/CD4⁺ T cell ratio was slightly increased (although not statistically significant) [Figure 6B].

Discussion

Here, we described the generation and characterization of a novel, fully human high-affinity antibody targeting the N-terminal domain of CEA. The parental clone G9 was isolated by phage display technology and showed specific binding to CEA, with a K_D of 640 nM. After two rounds of affinity maturation, we isolated the clone F4, which showed an almost 100-fold improvement in affinity compared to G9, with a K_D of 7.7 nM. F4 showed excellent biophysical properties *in vitro* and selectively stained CEA-positive cancer tissues in immunofluorescence.

CEA plays a crucial role in facilitating uncontrolled cell proliferation and metastasis through several mechanisms, including the dysregulation of transforming growth factor- β signaling,³⁸ inhibition of anoikis,³⁹ promotion of cell-cell adhesion, and binding to fibronectin.^{40–44} Notably, all these mechanisms are predominantly mediated by CEA(N).^{39,45,46}

Previous studies have demonstrated that inducing an immune response to CEA(N) or employing CEA(N)-binding aptamers can prevent tumor implantation *in vivo*.^{47,48} Thus, developing antibodies that target CEA(N) may be attractive for cancer therapy. However, the N-terminal domain is highly conserved between CEA and other CEACAMs, particularly CEACAM1 and CEACAM6. As the expression of these molecules is less tumor-specific,^{49,50} it is critical that CEA(N) targeting antibodies are not cross-reactive. This was demonstrated by flow cytometry on CHO cells expressing CEACAM1 and CEACAM6.

An *ex vivo*-based biodistribution analysis using FITC-labeled IgG antibodies and a quantitative biodistribution experiment with radiolabeled diabodies showed that a high-affinity clone is needed to achieve selective tumor accumulation. These results are in line with previous studies suggesting that tumor uptake can be improved by increasing the affinity to the single-digit nanomolar range.⁵¹ Interestingly, it was reported that increasing the affinity beyond the nanomolar range does not add to tumor accumulation but, in contrast, limits efficacious tumor penetration of antibodies as they get trapped by antigens at the rim of the tumor.⁵²

CEA is an attractive target for the treatment of mCRC, as virtually 100% of patients are strongly positive for the antigen.^{20,24–26} Although several CEA-targeting products have shown great potential in preclinical models,^{15,17,32,53}

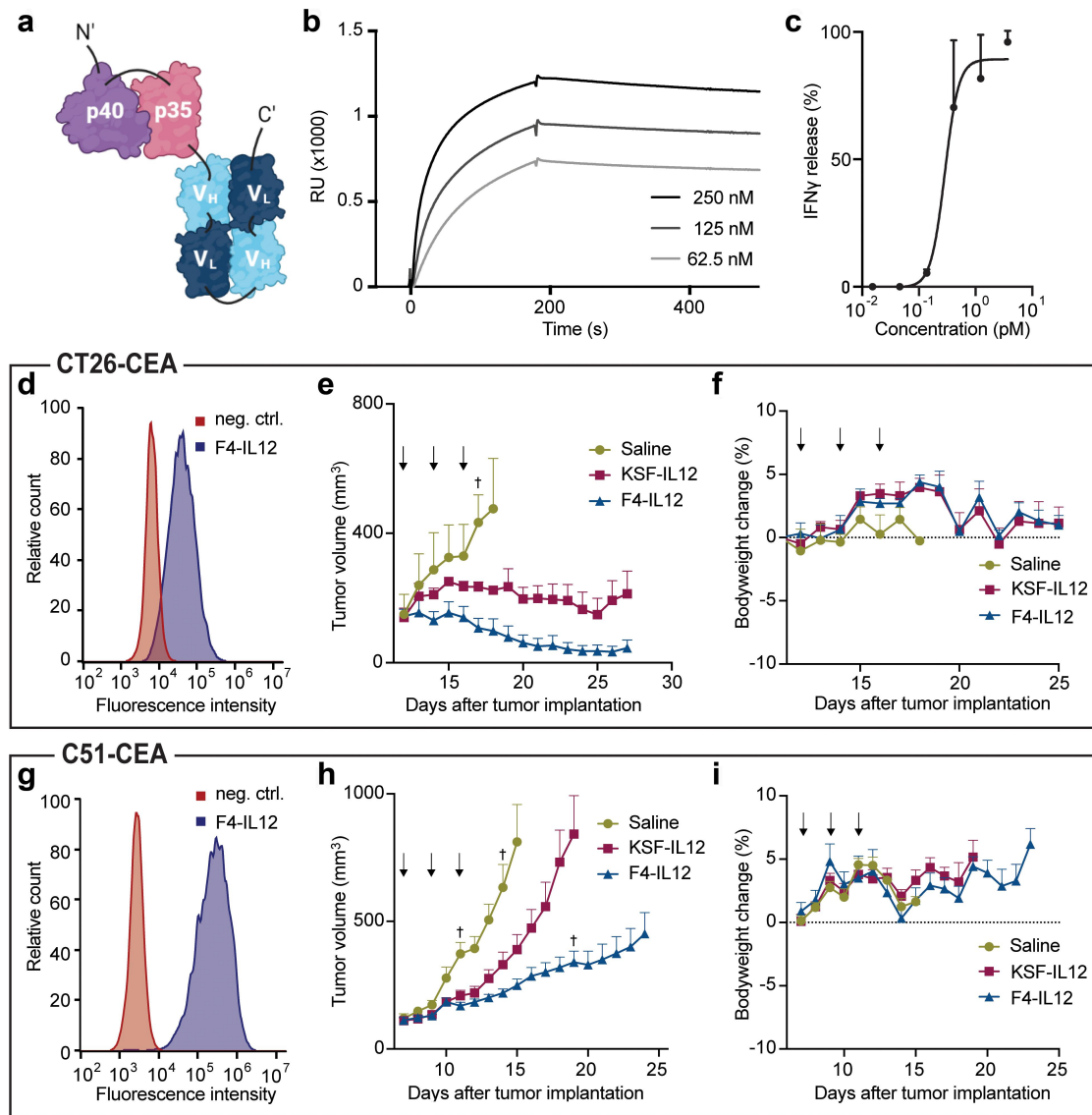


Figure 5. Preclinical characterization of F4-IL12. (a) Schematic representation of F4-IL12. P35 and p40 of murine IL12 were genetically linked to F4 in single-chain diabody format. (b) Surface plasmon analysis of F4-IL12 on recombinant CEA. (c) IFN γ release assay with F4-IL12 on murine splenocytes. (D and G) Flow cytometry analysis on CEA⁺ CT26 (d) and C51 (g) cells. As a negative control, cells were treated with the detecting secondary antibody only. (E and H) Tumor growth of (e) CT26-CEA bearing BALB/c mice treated with $3 \times 12 \mu\text{g}$ F4-IL12, KSF-IL12, or saline ($n = 3$) and (h) C51-CEA bearing BALB/c mice treated with the same compounds ($n = 8$). Mice were randomized when tumors reached an average volume of 100 mm^3 . Arrows indicate days of injection. †=mouse excluded due to ulceration. Bodyweight change of treated mice bearing (f) CT26-CEA tumors and (i) C51-CEA tumors. Error bars = SEM.

they were typically immunogenic and induced the development of ADAs in many patients.^{33,34,54} By focusing on the development of fully human antibodies isolated from a synthetic antibody library with short CDR3 loops, our group has previously generated and studied in the clinic antibody-cytokine fusion proteins, which were not immunogenic in patients.^{55,56} It is likely that the low immunogenic potential of those products may be due to the very low number of mutations in germline gene segments and to the use of wild-type cytokine sequences.

Recombinant human IL12 has been tested in the clinic against different cancer indications.^{57–61} However, systemic administration of IL12 induced life-threatening toxicities already at sub-optimal doses,^{62,63} preventing the escalation to therapeutically active regimens. It is becoming increasingly clear that the conjugation of certain cytokine payloads

to a tumor-targeting antibody moiety capable of selective homing to the neoplastic mass may represent an attractive strategy to improve the therapeutic index of this class of pharmaceuticals.⁶⁴ Many antibody-cytokine fusions are based on antibodies in IgG format. However, due to the interaction with the neonatal Fc receptor, prolonged circulatory half-life may increase the exposure of pro-inflammatory payloads to secondary lymphoid organs, thus enhancing the risk of cytokine-mediated toxicity. A number of research groups, including our own, have shown that antibody-fragment-based pharmacodelivery strategies may allow preferential localization at the tumor site, both in mice and in humans, reaching tumor:organ ratios as high as 20:1 twenty-four hours after intravenous administration.^{64–66} In line with those observations, the F4-IL12 fusion protein described here exhibited promising anti-cancer activity in

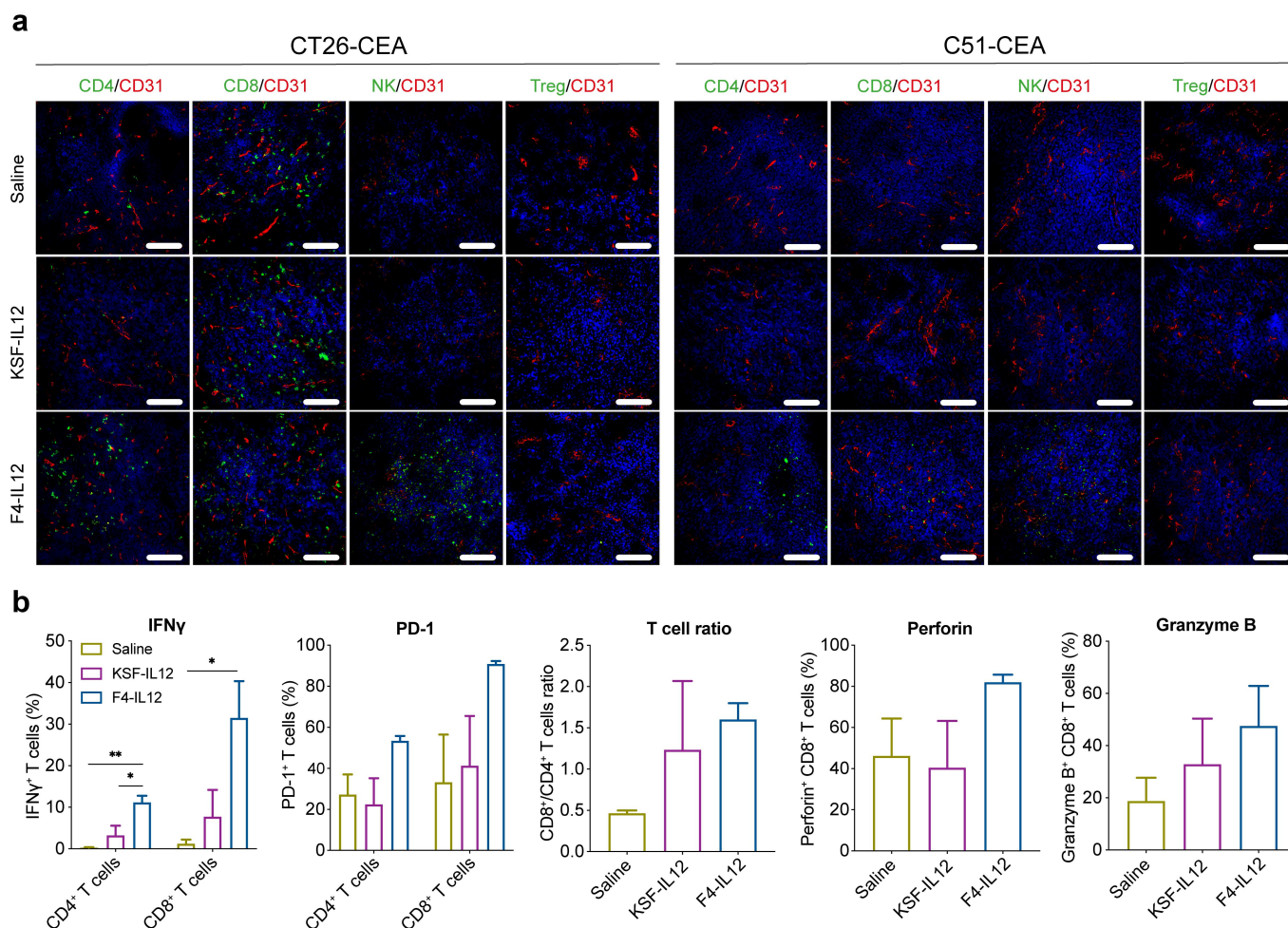


Figure 6. Ex vivo analysis of F4-IL12 treated tumor-bearing mice. (a) Analysis of tumor-infiltrating lymphocytes in CT26-CEA (left) and C51-CEA (right). Tumors were removed 48 hours after the third injection and analyzed by immunofluorescence staining. Markers specific for CD4⁺ T cells (CD4), CD8⁺ T cells (CD8), Natural killer cells (NKp46), and regulatory T cells (Foxp3) were used (green). Vasculature was visualized through CD31 staining (red) and nuclei with DAPI (blue). 20 \times magnification; scale bar = 100 μ m. (b) Phenotype analysis of CD4⁺ and CD8⁺ T cells in the tumor of treated C51-CEA bearing mice. Tumors were removed 48 hours after the third injection. Bar plots show expression levels of IFN γ , PD-1 (both in CD4⁺ and CD8⁺ T cells), the ratio of CD4⁺ and CD8⁺ T cells, and expression of Perforin and Granzyme B in CD8⁺ T cells. Statistical differences were assessed between mice receiving saline, KSF-IL12, and F4-IL12. * p < 0.05; ** p < 0.01 (regular one-way ANOVA test with Tukey posttest). Error bars = SEM; n = 3.

murine models of cancer at doses that were well tolerated. It is important to note that there is no direct murine equivalent of human CEA.⁶⁷ Consequently, the potential on-target side effects cannot be addressed with this study.

Ex vivo analysis of the neoplastic mass revealed that mice treated with F4-IL12 had an increased count of lymphocytes in the tumor and that tumor-homing T cells were more active compared to an IL12 fusion protein based on an antibody of irrelevant specificity in the mouse (KSF-IL12). F4-IL12 is now being considered for clinical development activities and may therefore represent an attractive combination partner to boost the activity of other immunomodulatory therapeutics, such as checkpoint inhibitors or bispecific antibodies since the performance of those pharmaceuticals relies on the presence of lymphocytes in the tumor.^{68–70} In general, the fully human F4 antibody may represent a useful tool for scientists who wish to use a non-immunogenic moiety as a delivery vehicle to target CEA-positive tumors in patients.

Materials and methods

Cell lines

CHO cells and the human colon adenocarcinomas LS174T, HT-29 were obtained from the American Type Culture Collection (ATCC). CEA-transfected CT26 and C51 cells were kindly provided by Dr. Bajic.⁵³ Cell lines were expanded and stored as cryopreserved aliquots in liquid nitrogen. Cells were grown following the supplier's protocol and kept in culture for no longer than 14 passages. The cell bank performed authentication of the cell line before shipment. It included: the evaluation of post-freeze viability, growth properties, and morphology, testing of mycoplasma contamination and sterility, and an isoenzyme assay.

Cloning and Expression of recombinant CEA

The synthetic cDNA encoding CEA(N) (UniProtKB P06731, position 35–150), flanked with an N-terminal AviTag (GLNDIFEAQKIEWHE) and a C-terminal 6-Histidine tag

was cloned into the mammalian cell expression vector pcDNA3.1(+) (ThermoFisher Scientific). The protein was expressed by polyethyleneimine (PEI)-induced transient gene expression (TGE) in CHO cells and purified by affinity chromatography using Ni-NTA agarose resin (Roche). Purified CEA(N) was dialyzed into phosphate-buffered saline (PBS; pH 7.4). The protein quality was analyzed by SDS-PAGE and SEC on a Superdex 75 Increase 75/150 GL column using an ÄKTA Pure FPLC (GE Healthcare). Before the SDS-PAGE, the protein was digested with PNGase F (New England BioLabs) under denaturing conditions to remove N-glycans.

CEA(N) was site-specifically biotin labeled on its AviTag, using BirA enzyme, following a previously described protocol.⁷¹ Biotinylation was validated through ELISA and a band shift assay.

Selection of antibodies by phage display and affinity maturation

Fully human monoclonal antibodies specific to CEA(N) were isolated by antibody phage display. Biotin-labeled CEA(N) was immobilized on streptavidin (SA)- (StreptaWells, Roche) or avidin-coated wells (Avidin [Sigma] on MaxiSorp plates [Sigma]). Antibodies specific to the CEA(N) antigen were enriched by two rounds of biopanning from a synthetic human scFv antibody library, as previously described by Viti et al.⁷² Individual clones infected with isolated phage were cultured, and scFv expression was induced by isopropyl β -D-1-thiogalactopyranoside. Bacterial supernatants containing antibody fragments were collected and screened by ELISA on immobilized CEA(N). Positive clones were analyzed by sequencing and used for further characterization. For each antibody, scFv and IgG fragments were cloned into a mammalian cell expression vector, expressed by TGE in CHO cells and purified by affinity chromatography, using protein A agarose (Thermo Scientific). Binding to the cognate antigen was confirmed by SPR, immunofluorescence, and flow cytometry analysis. The affinity of the best clone was improved by two rounds of affinity maturation, following the protocol described in Villa et al.⁷³ Briefly, new phage libraries were cloned by random mutagenesis of residues in the CDR1 or CDR2 loops of the V_H and V_L domains, and were subjected to one round of biopanning. Positive clones were selected by ELISA, and their binding kinetics were assessed by SPR.

Cloning, Expression, and Characterization of anti-CEA(N) Antibodies

All anti-CEA(N) antibodies used in this study were cloned and produced in-house. The DNA sequence of the positive control antibody Sm3E was obtained from Graff et al.⁷⁴ Genes for human IgG1 and murine IgG2a antibodies were cloned into the mammalian cell expression vector pMM137 (developed in-house). Genes for antibody fragments and antibody-cytokine fusions were cloned into the mammalian cell expression vector pcDNA3.1(+). Antibodies were produced by PEI-induced TGE in CHO cells, followed by purification to homogeneity by protein A affinity chromatography. Quality control of the produced antibodies was performed by SDS-PAGE and SEC

(Superdex 200 10/300GL or Superdex 75 10/300GL, GE Healthcare).

Surface plasmon resonance analysis

Biotinylated CEA(N) was immobilized on an SA-sensor chip with a density of 700 RU using a BIAcore X100 system (Cytiva). Real-time binding interactions were tested with serial dilutions of the antibodies at a flow rate of 10 μ l/min. Regeneration of the sensor chip was carried out by injecting 10 mM HCl. For the determination of the K_D, monomeric preparations of scFv were used. Analysis of the binding kinetics was performed on the BIAevaluation3.2 software.

Flow cytometry

LS174T cells, HT-29 cells, and CT26 cells were detached from the cell culture plate using Accutase cell detachment solution (Millipore). Cells were blocked for unspecific binding and stained with the anti-CEA antibody (IgG1). KSF IgG, binding to an irrelevant target, served as isotype control. Antibody binding was detected through a R-phycoerythrin (PE)-conjugated goat anti-human IgG Fc antibody (Invitrogen; TB28-2).

To test cross-reactivity toward the N-terminal domain of CEACAM1 and CEACAM6, CHO cells were transiently transfected using PEI and pcDNA3.1(+) vectors encoding full-length CEA (UniProtKB P06731), CEACAM1 (UniProtKB P13688), or CEACAM6 (UniProtKB P40199). Flow cytometry was performed 24 h after transfection. Briefly, cells were stained with the antibodies F4, Sm3E, or a positive control antibody (BioLegend; clone 5B2) in murine IgG2a format (50 nM). For detection, a PE-conjugated goat anti-mouse IgG antibody (Invitrogen; 12-4010-82) was used.

All staining and washing steps were carried out in cold FACS buffer (2% FBS, 2 mM EDTA in PBS; pH 7.4). Data was acquired on a CytoFLEX cytometer (Beckman Coulter) and the CytExpert software and processed with the FlowJo 10.4 software.

Immunofluorescence studies

Immunofluorescence analysis was performed on LS174T and HT-29 xenografts harvested from mice, on patient-derived colon cancer samples, and on a human tissue microarray (Amsbio, T6235700-5). Before staining, samples were fixed in ice-cold acetone. Sections were stained with FITC-labeled anti-CEA antibodies (IgG) at a concentration of 50 nM in 2% bovine serum albumin/PBS. KSF IgG-FITC, binding to hen egg lysozyme, served as isotype control. For detection, rabbit-anti-FITC antibody (Biorad; 4510-7804) and goat-anti-rabbit-Alexa Fluor488 (Invitrogen; A11008) were used. Tissue vasculature was visualized through CD31 (RD systems; RF3628 or Invitrogen; 14-0319-82) staining using an Alexa Fluor594-labeled secondary antibody (ThermoFisher; A11058 or Invitrogen; A11032). For the visualization of cell nuclei, DAPI (Invitrogen) was used. Slides were mounted with a fluorescence mounting medium (Dako Agilent) and analyzed with a Leika DMI6000B microscope (Leica Microsystems).

Ethical statement

Animal experiments were conducted according to the protocols approved by the Cantonal Veterinary Office Zurich (license number ZH006/21) in compliance with the Swiss Animal Protection Act (TSchG) and the Swiss Animal Protection Ordinance (TSchV).

Immunofluorescence-based biodistribution analysis

Eight weeks old female immunodeficient BALB/c nude mice were obtained from Janvier. Five million LS174T cells were injected subcutaneously into the right flank of each mouse. Tumors were grown to reach a volume of approximately 200 mm³ (volume = length x width²/2). Two hundred µg of FITC-labeled IgG antibodies were injected into the lateral tail vein. The mice were sacrificed 24 hours post-injection. The organs were excised and placed in a cryo-embedding medium (Thermo Scientific). Cryostat sections (12 µm) were stained and detected with rabbit anti-FITC (Biorad; 4510-7804) and anti-rabbit-Alexa Fluor488 (Invitrogen; A11008). Tissue vasculature was visualized through CD31 (RD systems; RF3628) staining using an Alexa Fluor594-labeled secondary antibody (ThermoFisher; A11058).

Quantitative biodistribution with radio-labeled diabodies

In vivo, tumor targeting was assessed by a quantitative biodistribution. 5 × 10⁶ LS174T cells were injected subcutaneously into the right flank of eight weeks old female immunodeficient BALB/c nude mice. Tumors were grown to reach a volume of approximately 200 mm³. G9, F7, F4, and KSF antibodies in diabodies format were radioiodinated with ¹²⁵I and chloramine T hydrate and purified on a PD10 column (Cytiva). Radiolabeled diabodies were injected into the lateral tail vein (*n* = 4). Mice were sacrificed 24 hours post-injection. Organs were excised and weighed, and radioactivity was counted using a Packard Cobra gamma counter (Packard, Meriden, CT, USA). Values are given as the percentage of injected dose per gram (ID/g).

Cloning, expression, and in vitro characterization of F4-IL12

The F4-IL12 fusion protein consists of the F4 antibody in single-chain diabody format fused to murine IL12. The gene was amplified by PCR and cloned into the mammalian cell expression vector pcDNA3.1 (+). The fusion protein was expressed in CHO cells, purified by affinity chromatography, and characterized as described above. The biological activity of IL12 was tested by an IFNγ release assay, as described by Puca et al.^{75,76} Binding to CEA was shown by SPR and flow cytometry as described above.

Therapy studies

CT26-CEA cells or C51-CEA cells were implanted subcutaneously into the right flank of eight weeks old female BALB/c mice. When tumors reached an average volume of 100 mm³, mice were randomized to achieve similar tumor volumes

between the study groups, and treatment was initiated by three intravenous injections of the tested protein (every 48 hours). Tumor growth and body weight change were monitored daily until the end of the study. Mice were euthanized if tumors reached a diameter of >15 mm or formed ulcers. The therapy studies were executed blinded.

Analysis of tumor-infiltrating lymphocytes

Eight weeks old female CT26-CEA and C51-CEA-bearing BALB/c mice were treated with the tested proteins, as described above. Forty-eight hours after the last injection, mice were euthanized, and tumors were excised and analyzed by immunofluorescence and flow cytometry.

For immunofluorescence, tumors were embedded in a cryo-embedding medium. Cryostat tissue sections (12 µm thickness) of each tumor were prepared. Immunofluorescence staining was carried out as described above. Tumor infiltrating lymphocytes were stained using the primary antibodies rat anti-Foxp3 (Invitrogen; 7000914), rat anti-NKp46 (BioLegend; 137602), rat anti-CD4 (Sino Biological; 50134-R001), and rat anti-CD8 (Sino Biological; 50389-R208), respectively. For detection, the secondary antibody donkey anti-rat Alexa Fluor488 (Invitrogen; A21208) was used. Vasculature was visualized through staining with goat anti-mouse CD31 (RD System; AF3628) and donkey anti-goat Alexa Fluor594 (Invitrogen; A21209) antibodies.

For flow cytometry analysis, tumors were digested in RPMI (supplemented with 10% FBS, 1 mg/mL type II collagenase, and 100 µg/mL DNase I) and filtered through a 70 µm cell strainer. Cell-surface staining was performed with the following antibodies (all purchased from BioLegend): CD45-FITC (C30-F11), CD4-PeCy7 (RM4-5), CD8-PerCP (53-6.7), and PD-1-BV421 (RMP1-30) (Panel 1) or CD45-FITC, CD8-PerCP, and NKp46-PE (Panel 2), followed by cell fixation in 4% PFA. For intracellular staining, cells were incubated with IFNγ-APC (XMG1.2) (Panel 1) or Granzyme B-APC (QA16A02) and Perforin-Pacific blue (S16009A) (Panel 2) in a permeabilization buffer (BioLegend). Cell viability was assessed with Zombie-NIR (BioLegend). Data were acquired and analyzed as described above.

Statistical analysis

Data were analyzed on Prism V.9.0 (GraphPad Software). Statistical significance between multiple groups was evaluated by one-way analysis of variance (ANOVA) followed by Tukey's posttest. Differences in tumor growth were compared by two-way ANOVA followed by Tukey's posttest. *P* < 0.05 was considered statistically significant.

Acknowledgments

The authors thank Gudrun Thorhallsdottir, Mattia Matasci, Baptiste Gouyou, and Anne Kerschenmeyer for their help with experimental procedures. The authors thank ScopeM (ETH Zürich) for the use of their electron microscopy facilities.

Authors contributions

Conception and design: L.P., R.D., E.P., D.N.

Development of methodology: L.P., G.R., A.V., R.D., E.P., D.N.

Acquisition of data: L.P., F.P., J.R., A.E., G.R., R.D.

Analysis and interpretation of data: L.P., F.P., J.R., A.E., G.R., S.D.P., A.V., R.D., E.P., A.O., D.N.

Study supervision: A.V., A.O., R.D., D.N.

Disclosure statement

Dario Neri is a co-founder and shareholder of Philogen (www.philogen.com), a Swiss-Italian Biotech company that operates in the field of ligand-based pharmacodelivery. Louis Plüss, Frederik Peisert, Abdullah Elsayed, Sheila Dakhel Plaza, Emanuele Puca, and Roberto De Luca are employees of Philochem AG, a daughter company of Philogen acting as the discovery unit of the group.

Funding

This research received no external funding.

ORCID

Louis Plüss  <http://orcid.org/0009-0003-6426-7249>

Frederik Peisert  <http://orcid.org/0000-0002-1856-8118>

Abdullah Elsayed  <http://orcid.org/0000-0001-7080-0853>

Giulia Rotta  <http://orcid.org/0000-0001-6897-9225>

Sheila Dakhel Plaza  <http://orcid.org/0000-0003-2546-6053>

Alessandra Villa  <http://orcid.org/0000-0003-4070-286X>

Emanuele Puca  <http://orcid.org/0000-0002-2869-3203>

Annette Oxenius  <http://orcid.org/0000-0002-2079-2354>

Dario Neri  <http://orcid.org/0000-0001-5234-7370>

Availability of data and materials

Most of the data that supports the findings of this study are available in the supplementary material of this article. The remaining data that support the findings of this study are available from the corresponding author upon reasonable request.

Abbreviations

ADA	Anti-drug antibody
ATCC	American Type Culture Collection
CDR	Complementarity-determining region
CEA	Carcinoembryonic antigen
CEACAM	Carcinoembryonic antigen-related cell adhesion molecule
CEA(N)	N-terminal domain of CEA
CHO	Chinese Hamster Ovary
CRC	Colorectal Cancer
DAPI	4',6-diamidino-2-phenylindole
EDTA	Ethylenediaminetetraacetic acid
ELISA	Enzyme-linked immunosorbent assay
FITC	Fluorescein isothiocyanate
FPLC	Fast protein liquid chromatography
IFN	Interferon
IL	Interleukin
K _D	Dissociation constant
mCRC	Metastatic colorectal cancer
Ni-NTA	Nickel nitrilotriacetic acid
NK	Natural killer
PBS	Phosphate-Buffered Saline
PCR	Polymerase Chain Reaction
PE	R-phycoerythrin
PEI	Polyethyleneimine
SA	Streptavidin

scFv	Single chain variable fragment
SDS-PAGE	Sodium dodecyl sulfate-polyacrylamide gel electrophoresis
SEC	Size exclusion chromatography
SPR	Surface plasmon resonance
V _H	Variable heavy
V _L	Variable light

References

- Bray F, Ferlay J, Soerjomataram I, Siegel RL, Torre LA, Jemal A. Global cancer statistics 2018: gLOBOCAN estimates of incidence and mortality worldwide for 36 cancers in 185 countries. *CA Cancer J Clin.* 2018;68(6):394–424. doi:<https://doi.org/10.3322/caac.21492>.
- Issa IA, Nouredine M. Colorectal cancer screening: an updated review of the available options. *World J Gastroenterol.* 2017;23(28):5086–96. PMID: 28811705. doi:[10.3748/wjg.v23.i28.5086](https://doi.org/10.3748/wjg.v23.i28.5086).
- Riihimäki M, Hemminki A, Sundquist J, Hemminki K. Patterns of metastasis in colon and rectal cancer. *null.* 2016;6(1):29765. doi:[10.1038/srep29765](https://doi.org/10.1038/srep29765).
- Biller LH, Schrag D. Diagnosis and treatment of metastatic colorectal cancer: a review. *Jama.* 2021;325(7):669–85. PMID: 33591350. doi:[10.1001/jama.2021.0106](https://doi.org/10.1001/jama.2021.0106).
- Cancer Stat Facts: Colorectal Cancer. National Cancer Institute; Surveillance, Epidemiology, and End Results Program: Maryland (MD); 2012–2018; [accessed Mar 28] <https://seer.cancer.gov/statfacts/html/colorect.html>
- Coupez D, Hulo P, Toucheffeu Y, Bossard C, Bennouna J. Pembrolizumab for the treatment of colorectal cancer. *Expert Opin Biol Ther.* 2020;20(3):219–26. PMID: 31952453. doi:[10.1080/14712598.2020.1718095](https://doi.org/10.1080/14712598.2020.1718095).
- Eggermont AMM, Blank CU, Mandala M, Long GV, Atkinson V, Dalle S, Haydon A, Lichinitser M, Khattak A, Carlino MS, et al. Adjuvant pembrolizumab versus placebo in resected stage iii melanoma. *N Engl J Med.* 2018;378(19):1789–801. doi:[10.1056/NEJMoa1802357](https://doi.org/10.1056/NEJMoa1802357). PMID: 29658430.
- Choueiri TK, Fishman MN, Escudier B, McDermott DF, Drake CG, Kluger H, Stadler WM, Perez-Gracia JL, McNeel DG, Curti B, et al. Immunomodulatory activity of nivolumab in metastatic renal cell carcinoma. *Clin Cancer Res.* 2016;22(22):5461–71. doi:[10.1158/1078-0432.Ccr-15-2839](https://doi.org/10.1158/1078-0432.Ccr-15-2839). PMID: 27169994.
- Garon EB, Rizvi NA, Hui R, Leigh N, Balmanoukian AS, Eder JP, Patnaik A, Aggarwal C, Gubens M, Horn L, et al. Pembrolizumab for the treatment of non-small-cell lung cancer. *N Engl J Med.* 2015;372(21):2018–28. doi:[10.1056/NEJMoa1501824](https://doi.org/10.1056/NEJMoa1501824). PMID: 25891174.
- Sundar R, Cho B-C, Brahmer JR, Soo RA. Nivolumab in NSCLC: latest evidence and clinical potential. *Ther Adv Med Oncol.* 2015;7(2):85–96. doi:[10.1177/1758834014567470](https://doi.org/10.1177/1758834014567470).
- Topalian SL, Hodi FS, Brahmer JR, Gettinger SN, Smith DC, McDermott DF, Powderly JD, Carvajal RD, Sosman JA, Atkins MB, et al. Safety, activity, and immune correlates of anti-PD-1 antibody in cancer. *N Engl J Med.* 2012;366(26):2443–54. doi:[10.1056/NEJMoa1200690](https://doi.org/10.1056/NEJMoa1200690). PMID: 22658127.
- Arora SP, Mahalingam D. Immunotherapy in colorectal cancer: for the select few or all? *J Gastrointest Oncol.* 2018;9(1):170–79. PMID: 29564183. doi:[10.21037/jgo.2017.06.10](https://doi.org/10.21037/jgo.2017.06.10).
- Lu R-M, Hwang Y-C, Liu I-J, Lee C-C, Tsai H-Z, Li H-J, Wu H-C. Development of therapeutic antibodies for the treatment of diseases. *J Biomed Sci.* 2020;27(1):1. doi:[10.1186/s12929-019-0592-z](https://doi.org/10.1186/s12929-019-0592-z).
- Murer P, Neri D. Antibody-cytokine fusion proteins: a novel class of biopharmaceuticals for the therapy of cancer and of chronic inflammation. *N Biotechnol.* 2019;52:42–53. doi:[10.1016/j.nbt.2019.04.002](https://doi.org/10.1016/j.nbt.2019.04.002).
- Puca E, Schmitt-Koopmann C, Furter M, Murer P, Probst P, Dühr M, Bajic D, Neri D. The targeted delivery of interleukin-12 to the carcinoembryonic antigen increases the intratumoral density of NK and CD8(+) T cell in an immunocompetent mouse

- model of colorectal cancer. *J Gastrointest Oncol.* 2020;11(4):803–11. PMID: 32953162. doi:10.21037/jgo.2020.04.02.
16. Schwegler C, Dorn-Beineke A, Nittka S, Stocking C, Neumaier M. Monoclonal anti-idiotype antibody 6G6.C4 Fused to GM-CSF is capable of breaking tolerance to carcinoembryonic antigen (CEA) in CEA-transgenic mice. *Cancer Res.* 2005;65(5):1925–33. doi:10.1158/0008-5472.Can-04-3591.
 17. Klein C, Waldhauer I, Nicolini VG, Freimoser-Grundschober A, Nayak T, Vugts DJ, Dunn C, Bolijn M, Benz J, Stihle M, et al. Cergutuzumab amunaleukin (CEA-IL2v), a CEA-targeted IL-2 variant-based immunocytokine for combination cancer immunotherapy: overcoming limitations of aldesleukin and conventional IL-2-based immunocytokines. *OncoImmunology.* 2017;6(3):e1277306. doi:10.1080/2162402X.2016.1277306.
 18. Bacac M, Fauti T, Sam J, Colombetti S, Weinzierl T, Ouaret D, Bodmer W, Lehmann S, Hofer T, Hosse RJ, et al. A novel carcinoembryonic antigen T-Cell Bispecific Antibody (CEA TCB) for the treatment of solid tumors. *Clin Cancer Res.* 2016;22(13):3286–97. doi:10.1158/1078-0432.Ccr-15-1696.
 19. Gauthier L, Morel A, Anceriz N, Rossi B, Blanchard-Alvarez A, Grondin G, Trichard S, Cesari C, Sapet M, Bosco F, et al. Multifunctional natural killer cell engagers targeting NKp46 trigger protective tumor immunity. *Cell.* 2019;177(7):1701–13. e1716. doi:https://doi.org/10.1016/j.cell.2019.04.041.
 20. Tiernan JP, Perry SL, Verghese ET, West NP, Yeluri S, Jayne DG, Hughes TA. Carcinoembryonic antigen is the preferred biomarker for in vivo colorectal cancer targeting. *Br J Cancer.* 2013;108(3):662–67. doi:10.1038/bjc.2012.605.
 21. Hammarström S, Baranov V. Is there a role for CEA in innate immunity in the colon? *Trends Microbiol.* 2001;9(3):119–25. doi:https://doi.org/10.1016/S0966-842X(01)01952-7.
 22. Nap M, Mollgard K, Burtin P, Fleuren GJ. Immunohistochemistry of carcino-embryonic antigen in the embryo, fetus and adult. *Tumor Biol.* 1988;9(2–3):145–53. doi:10.1159/000217555.
 23. Hammarström S. The carcinoembryonic antigen (CEA) family: structures, suggested functions and expression in normal and malignant tissues. *Semin Cancer Biol.* 1999;9:67–81. doi:10.1006/scbi.1998.0119.
 24. Rousseau C, Goldenberg DM, Colombié M, Sébille J-C, Meingan P, Ferrer L, Baumgartner P, Cerato E, Masson D, Campone M, et al. Initial clinical results of a novel immuno-PET theranostic probe in human epidermal growth factor receptor 2-negative breast cancer. *J Nucl Med.* 2020;61(8):1205–11. doi:10.2967/jnumed.119.236000.
 25. Bodet-Milin C, Bailly C, Toucheffeu Y, Frampas E, Bourgeois M, Rauscher A, Lacoëuille F, Drui D, Arlicot N, Goldenberg DM, et al. Clinical results in medullary thyroid carcinoma suggest high potential of pretargeted immuno-PET for tumor imaging and theranostic approaches. *Front Med.* 2019;6:124. doi:10.3389/fmed.2019.00124.
 26. Schoffelen R, Boerman OC, Goldenberg DM, Sharkey RM, van Herpen CM, Franssen GM, McBride WJ, Chang C-H, Rossi EA, van der Graaf WT, et al. Development of an imaging-guided CEA-pretargeted radionuclide treatment of advanced colorectal cancer: first clinical results. *Br J Cancer.* 2013;109(4):934–42. doi:10.1038/bjc.2013.376.
 27. Hao C, Zhang G, Zhang L. Serum CEA levels in 49 different types of cancer and noncancer diseases. *Prog Mol Biol Transl Sci.* 2019;162:213–27.
 28. Chester KA, Begent R. Circulating immune complexes (CIC), carcinoembryonic antigen (CEA) and CIC containing CEA as markers for colorectal cancer. *Clin Exp Immunol.* 1984;58:685.
 29. Liersch T, Meller J, Bittrich M, Kulle B, Becker H, Goldenberg DM. Update of carcinoembryonic antigen radioimmunotherapy with 131 I-labetuzumab after salvage resection of colorectal liver metastases: comparison of outcome to a contemporaneous control group. *Ann Surg Oncol.* 2007;14(9):2577–90. doi:10.1245/s10434-006-9328-x.
 30. Dotan E, Cohen SJ, Starodub AN, Lieu CH, Messersmith WA, Simpson PS, Guarino MJ, Marshall JL, Goldberg RM, Hecht JR, et al. Phase I/II trial of labetuzumab govitecan (anti-CEACAM5/SN-38 antibody-drug conjugate) in patients with refractory or relapsing metastatic colorectal cancer. *J Clin Oncol.* 2017;35(29):3338. doi:10.1200/JCO.2017.73.9011.
 31. Lutterbueser R, Raum T, Kischel R, Lutterbueser P, Schlereth B, Schaller E, Mangold S, Rau D, Meier P, Kiener PA, et al. Potent control of tumor growth by CEA/CD3-bispecific single-chain antibody constructs that are not competitively inhibited by soluble CEA. *J Immunother.* 2009;32(4):341–52. doi:10.1097/CJI.0b013e31819b7c70.
 32. Oberst MD, Fuhrmann S, Mulgrew K, Amann M, Cheng L, Lutterbueser P, Richman L, Coats S, Baeuerle PA, Hammond SA. CEA/CD3 bispecific antibody MEDI-565/AMG 211 activation of T cells and subsequent killing of human tumors is independent of mutations commonly found in colorectal adenocarcinomas. *mAbs.* 2014;6(6): 1571–84.
 33. Pishvaian MJ, Morse M, McDevitt JT, Ren S, Robbie G, Ryan PC, Soukharev S, Bao H, Denlinger CS. Phase 1 dose escalation study of MEDI-565, a bispecific T-cell engager that targets human carcinoembryonic antigen (CEA), in patients with advanced gastrointestinal (GI) adenocarcinomas. In: phase 1 dose escalation study of MEDI-565, a bispecific T-cell engager that targets human carcinoembryonic antigen (CEA), in patients with advanced gastrointestinal (GI) adenocarcinomas. *Am J Clin Oncol.* 2016;15(4):345–51.
 34. Moek K, Fiedler W, von Einem J, Verheul H, Seufferlein T, de Groot D, Heinemann V, Kebenko M, Menke-van der Houven van Oordt CW, Ettrich TJ, et al. Phase I study of AMG 211/MEDI-565 administered as continuous intravenous infusion (cIV) for relapsed/refractory gastrointestinal (GI) adenocarcinoma. *Ann Oncol.* 2018;29:viii139–40. doi:10.1093/annonc/mdy279.414.
 35. Murer P, Plüss L, Neri D. A novel human monoclonal antibody specific to the A33 glycoprotein recognizes colorectal cancer and inhibits metastasis. *mAbs.* 2020;12(1): 1714371.
 36. Nadal L, Corbellari R, Villa A, Weiss T, Weller M, Neri D, De Luca R. Novel human monoclonal antibodies specific to the alternatively spliced domain D of Tenascin C efficiently target tumors in vivo. *mAbs.* 2020;12(1): 1836713.
 37. Hutmacher C, Volta L, Rinaldi F, Murer P, Myburgh R, Manz MG, Neri D. Development of a novel fully-human anti-CD123 antibody to target acute myeloid leukemia. *Leuk Res.* 2019;84:106178. doi:10.1016/j.leukres.2019.106178.
 38. Li Y, Cao H, Jiao Z, Pakala SB, Sirigiri DN, Li W, Kumar R, Mishra L. Carcinoembryonic antigen interacts with TGF- β receptor and inhibits TGF- β signaling in colorectal cancers. *Cancer Res.* 2010;70(20):8159–68. PMID: 20889724. doi:10.1158/0008-5472.Can-10-1073.
 39. Ordoñez C, Screaton RA, Ilantzis C, Stanners CP. Human carcinoembryonic antigen functions as a general inhibitor of anoiniks. *Cancer Res.* 2000;60(13):3419–24. PMID: 10910050.
 40. Benchimol S, Fuks A, Jothy S, Beauchemin N, Shirota K, Stanners CP. Carcinoembryonic antigen, a human tumor marker, functions as an intercellular adhesion molecule. *Cell.* 1989;57(2):327–34. PMID: 2702691. doi:10.1016/0092-8674(89)90970-7.
 41. Taheri M, Saragovi U, Fuks A, Makkerh J, Mort J, Stanners CP. Self Recognition in the Ig Superfamily: IDENTIFICATION OF PRECISE SUBDOMAINS in CARCINOEMBRYONIC ANTIGEN REQUIRED for INTERCELLULAR ADHESION*. *J Biol Chem.* 2000;275(35):26935–43. doi:https://doi.org/10.1016/S0021-9258(19)61463-8.
 42. Thomas P, Forse RA, Bajenova O. Carcinoembryonic antigen (CEA) and its receptor hnRNP M are mediators of metastasis and the inflammatory response in the liver. *Clin Exp Metastasis.* 2011;28(8):923–32. PMID: 21901530. doi:10.1007/s10585-011-9419-3.
 43. Ordonez C, Zhai AB, Camacho-Leal P, Demarte L, Fan MM, Stanners CP. GPI-anchored CEA family glycoproteins CEA and CEACAM6 mediate their biological effects through enhanced integrin $\alpha 5 \beta 1$ -fibronectin interaction. *J Cell Physiol.* 2007;210(3):757–65. PMID: 17167768. doi:10.1002/jcp.20887.

44. Camacho-Leal P, Zhai AB, Stanners CP. A co-clustering model involving $\alpha 5\beta 1$ integrin for the biological effects of GPI-anchored human carcinoembryonic antigen (CEA). *J Cell Physiol.* 2007;211(3):791–802. PMID: 17286276. doi:10.1002/jcp.20989.
45. Samara RN, Laguigne LM, Jessup JM. Carcinoembryonic antigen inhibits anoikis in colorectal carcinoma cells by interfering with TRAIL-R2 (DR5) signaling. *Cancer Res.* 2007;67(10):4774–82. PMID: 17510406. doi:10.1158/0008-5472.Can-06-4315.
46. Abdul-Wahid A, Huang EH, Cydzik M, Bolewska-Pedyczak E, Gariépy J. The carcinoembryonic antigen IgV-like N domain plays a critical role in the implantation of metastatic tumor cells. *Mol Oncol.* 2014;8(2):337–50. PMID: 24388361. doi:10.1016/j.molonc.2013.12.002.
47. Abdul-Wahid A, Huang EH, Lu H, Flanagan J, Mallick AI, Gariépy J. A focused immune response targeting the homotypic binding domain of the carcinoembryonic antigen blocks the establishment of tumor foci in vivo. *Int J Cancer.* 2012;131(12):2839–51. PMID: 22495743. doi:10.1002/ijc.27582.
48. Orava EW, Abdul-Wahid A, Huang EH, Mallick AI, Gariépy J. Blocking the attachment of cancer cells in vivo with DNA aptamers displaying anti-adhesive properties against the carcinoembryonic antigen. *Mol Oncol.* 2013;7(4):799–811. PMID: 23656757. doi:10.1016/j.molonc.2013.03.005.
49. Schölzel S, Zimmermann W, Schwarzkopf G, Grunert F, Rogaczewski B, Thompson J. Carcinoembryonic antigen family members CEACAM6 and CEACAM7 are differentially expressed in normal tissues and oppositely deregulated in hyperplastic colorectal polyps and early adenomas. *Am J Pathol.* 2000;156(2):595–605. PMID: 10666389. doi:10.1016/s0002-9440(10)64764-5.
50. Prall F, Nollau P, Neumaier M, Haubeck HD, Drzeniek Z, Helmchen U, Löning T, Wagener C. Cd66a (BGP), an adhesion molecule of the carcinoembryonic antigen family, is expressed in epithelium, endothelium, and myeloid cells in a wide range of normal human tissues. *J Histochem Cytochem.* 1996;44(1):35–41. PMID: 8543780. doi:10.1177/44.1.8543780.
51. Adams GP, Schier R, McCall AM, Simmons HH, Horak EM, Alpaugh RK, Marks JD, Weiner LM. High affinity restricts the localization and tumor penetration of single-chain fv antibody molecules. *Cancer Res.* 2001;61(12):4750–55. PMID: 11406547.
52. Rudnick SI, Lou J, Shaller CC, Tang Y, Klein-Szanto AJ, Weiner LM, Marks JD, Adams GP. Influence of affinity and antigen internalization on the uptake and penetration of Anti-HER2 antibodies in solid tumors. *Cancer Res.* 2011;71(6):2250–59. PMID: 21406401. doi:10.1158/0008-5472.Can-10-2277.
53. Bajic D, Chester K, Neri D. An antibody-tumor necrosis factor fusion protein that synergizes with oxaliplatin for treatment of colorectal cancer immunocytokine synergizes with oxaliplatin in cancer models. *Mol Cancer Ther.* 2020;19(12):2554–63. doi:10.1158/1535-7163.MCT-19-0729.
54. van Brummelen EMJ, Huisman MC, de Wit-van der Veen LJ, Nayak TK, Stokkel MPM, Mulder ER, Hoekstra OS, Vugts DJ, Van Dongen G, Verheul HM, et al. (89)zr-labeled CEA-targeted IL-2 variant immunocytokine in patients with solid tumors: cEA-mediated tumor accumulation and role of IL-2 receptor-binding. *Oncotarget.* 2018;9(37):24737–49. doi:10.18632/oncotarget.25343. PMID: 29872502.
55. Spitaleri G, Berardi R, Pierantoni C, De Pas T, Noberasco C, Libbra C, González-Iglesias R, Giovannoni L, Tasciotti A, Neri D, et al. Phase I/II study of the tumour-targeting human monoclonal antibody-cytokine fusion protein L19-TNF in patients with advanced solid tumours. *J Cancer Res Clin Oncol.* 2013;139(3):447–55. doi:10.1007/s00432-012-1327-7. PMID: 23160853.
56. Curigliano G, Spitaleri G, De Pas T, Noberasco C, Giovannoni L, Messen H, Zardi L, Milani A, Neri D, De Braud F. A dose finding pharmacokinetic study of the tumor-targeting human L19-IL2 monoclonal antibody-cytokine fusion protein in patients with advanced solid tumors. *J Clin Oncol.* 2007;25(18_suppl):3057–3057. doi:10.1200/jco.2007.25.18_suppl.3057.
57. Guida M, Casamassima A, Monticelli G, Quaranta M, Colucci G. Basal cytokines profile in metastatic renal cell carcinoma patients treated with subcutaneous IL-2-based therapy compared with that of healthy donors. *J Transl Med.* 2007;5(1):51. PMID: 17953739. doi:10.1186/1479-5876-5-51.
58. Ansell SM, Witzig TE, Kurtin PJ, Sloan JA, Jelinek DF, Howell KG, Markovic SN, Habermann TM, Klee GG, Atherton PJ, et al. Phase I study of interleukin-12 in combination with rituximab in patients with B-cell non-Hodgkin lymphoma. *Blood.* 2002;99(1):67–74. doi:10.1182/blood.v99.1.67. PMID: 11756154.
59. Little RF, Pluda JM, Wyvill KM, Rodriguez-Chavez IR, Tosato G, Catanzaro AT, Steinberg SM, Yarchoan R. Activity of subcutaneous interleukin-12 in AIDS-related Kaposi sarcoma. *Blood.* 2006;107(12):4650–57. PMID: 16507779. doi:10.1182/blood-2005-11-4455.
60. Nunez A, Arroyo N, Godoy L, Dutil J. The role of interleukin-12 in breast cancer (CCR6P. 220). *J Immunol.* 2015;194(1_Supplement):187.187–187.187. doi:10.4049/jimmunol.194.Supp.187.7.
61. Rook AH, Wood GS, Yoo EK, Elenitsas R, Kao DM, Sherman ML, Witmer WK, Rockwell KA, Shane RB, Lessin SR, et al. Interleukin-12 therapy of cutaneous T-cell lymphoma induces lesion regression and cytotoxic T-cell responses. *Blood J Am Society Hematol.* 1999;94(3):902–08. doi:10.1182/blood.V94.3.902.415k23_902_908.
62. Portielje JE, Kruijth WH, Schuler M, Beck J, Lamers CH, Stoter G, Huber C, de Boer-Dennert M, Rakhit A, Bolhuis RL, et al. Phase I study of subcutaneously administered recombinant human interleukin 12 in patients with advanced renal cell cancer. *Clin Cancer Res.* 1999;5(12):3983–89. PMID: 10632329.
63. Leonard JP, Sherman ML, Fisher GL, Buchanan LJ, Larsen G, Atkins MB, Sosman JA, Dutcher JP, Vogelzang NJ, Ryan JL. Effects of single-dose interleukin-12 exposure on interleukin-12-associated toxicity and interferon- γ production. *Blood J Am Society Hematol.* 1997;90:2541–48.
64. Neri D. Antibody-cytokine fusions: versatile products for the modulation of anticancer immunity. *Cancer Immunol Res.* 2019;7(3):348–54. doi:10.1158/2326-6066.CIR-18-0622.
65. Poli GL, Bianchi C, Virota G, Bettini A, Moretti R, Trachsel E, Elia G, Giovannoni L, Neri D, Bruno A. Radretumab radioimmunotherapy in patients with brain metastasis: a 124I-L19SIP Dosimetric PET Study/124I-L19SIP PET Study in Patients with Brain Metastasis. *Cancer Immunol Res.* 2013;1:134–43.
66. Erba PA, Sollini M, Orciuolo E, Traino C, Petrini M, Paganelli G, Bombardieri E, Grana C, Giovannoni L, Neri D, et al. Radioimmunotherapy with radretumab in patients with relapsed hematologic malignancies. *J Nucl Med.* 2012;53(6):922–27. doi:10.2967/jnumed.111.101006.
67. Chan CHF, Stanners CP. Novel mouse model for carcinoembryonic antigen-based therapy. *Mol Ther.* 2004;9(6):775–85. doi:https://doi.org/10.1016/j.ymthe.2004.03.009.
68. Sam J, Colombetti S, Fauti T, Roller A, Biehl M, Fahrni L, Nicolini V, Perro M, Nayak T, Bommer E, et al. Combination of T-cell bispecific antibodies with PD-L1 checkpoint inhibition elicits superior anti-tumor activity. *Front Oncol.* 2020;10:575737. doi:10.3389/fonc.2020.575737.
69. Claus C, Ferrara C, Xu W, Sam J, Lang S, Uhlenbrock F, Albrecht R, Herter S, Schlenker R, Hüsser T, et al. Tumor-targeted 4-1BB agonists for combination with T cell bispecific antibodies as off-the-shelf therapy. *Sci Transl Med.* 2019;11(496):eaav5989. doi:10.1126/scitranslmed.aav5989.
70. Liu YT, Sun ZJ. Turning cold tumors into hot tumors by improving T-cell infiltration. *Theranostics.* 2021;11(11):5365–86. PMID: 33859752. doi:10.7150/thno.58390.
71. Fairhead M, Howarth M. Site-specific biotinylation of purified proteins using BirA. *Methods Mol Biol.* 2015;216(7):171–84.
72. Viti F, Nilsson F, Demartis S, Huber A, Neri D. Design and use of phage display libraries for the selection of antibodies and enzymes. *Methods Enzymol.* 2000;326:480–505. PMID: 11036659. doi:10.1016/s0076-6879(00)26071-0.

73. Villa A, Trachsel E, Kaspar M, Schliemann C, Somavilla R, Rybak JN, Röslı C, Borsi L, Neri D. A high-affinity human monoclonal antibody specific to the alternatively spliced EDA domain of fibronectin efficiently targets tumor neo-vasculature in vivo. *Int J Cancer*. 2008;122(11):2405–13. PMID: 18271006. doi:10.1002/ijc.23408.
74. Graff CP, Chester K, Begent R, Wittrup KD. Directed evolution of an anti-carcinoembryonic antigen scFv with a 4-day monovalent dissociation half-time at 37 C. *Protein Eng Des Sel*. 2004;17(4):293–304. PMID: 15115853. doi:10.1093/protein/gzh038.
75. Puca E, Probst P, Stringhini M, Murer P, Pellegrini G, Cazzamalli S, Huttmacher C, Gouyou B, Wulhfard S, Matasci M, et al. The antibody-based delivery of interleukin-12 to solid tumors boosts NK and CD8 + T cell activity and synergizes with immune checkpoint inhibitors. *Int J Cancer*. 2020;146(9):2518–30. doi:10.1002/ijc.32603. PMID: 31374124.
76. Tomlinson IM, Cox JP, Gherardi E, Lesk AM, Chothia C. The structural repertoire of the human V kappa domain. *Embo J*. 1995;14(18):4628–38. PMID: 7556106. doi:10.1002/j.1460-2075.1995.tb00142.x.